ZOOLOGICAL SCIENCE **25**: 129–138 (2008)

Large-Scale Identification by Shotgun Proteomics of Proteins Expressed in Porcine Liver and Salivary Gland

Tomoyo Tsujita[1†], DukJin Kang[2†], Myeong Hee Moon[2], Nobuhiro Ohno[1], Tadao Inoue[1], Mitsuhito Matsumoto[3], Yuji Kaji[3] and Yasunori Yamaguchi[1]*

[1]*Department of Biotechnology, Fukuyama University, Fukuyama 729-0292, Japan*
[2]*Department of Chemistry, Yonsei University, Seoul 120-749, Korea*
[3]*National Agricultural Research Center for Kyushu Okinawa Region, Kumamoto 861-1192, Japan*

Protein catalogs containing a large number of proteins expressed in a variety of organs can be powerful tools for stem-cell research, because this requires accurate knowledge about how cells differentiate. Salivary gland progenitor (SGP) cells are somatic stem cells isolated from the salivary gland that can differentiate into hepatic or pancreatic cell lineages. Their differentiation state has been assessed by the expression of major protein markers, but to use these cells in regenerative medicine, it will be necessary to establish additional means of quality assessment. We examined the use of shotgun proteomics for porcine salivary gland (a source of SGP cells) and liver (a destination of differentiated SGP cells) for determining the state of SGP cell differentiation. Protein complexes from each organ were digested into peptides and separated by two-dimensional liquid chromatography involving strong cation-exchange chromatography followed by reversed-phase liquid chromatography. The separated peptides were analyzed by on-line electrospray ionization tandem mass spectrometry using a quadrupole-time of flight mass spectrometer (ESI Q-TOF MS/MS), and the spectra obtained were processed to search peptides against a mammalian database for protein identification. Using this method, we identified 117 proteins in porcine salivary gland and 154 proteins in porcine liver. Of these, 72 and 109 were specific to salivary gland and liver, respectively, and some of these were previously shown to be organ specific. The current study can be utilized in the future as a basis to study the pattern of differentiation in protein expression by stem cells.

Key words: porcine, shotgun proteomics, SGP, SCX-RPLC separation, tandem mass spectrometry

INTRODUCTION

The liver is one of the most complex organs in animals, and it plays critical roles during development, including the detoxification of xenobiotics, the metabolism of lipids and sugars, and the purification of blood (Kellum et al., 2003; Naruse, 2005; Sarlis and Gourgiotis, 2005). Although many liver-related diseases have been reported, liver transplantation has for many years been the only way to effectively treat severe liver diseases (Brown and Moonka, 2004; Shimada et al., 2005); however, the lack of enough donors for a large number of patients and immunorejection represents major challenges.

One idea to alleviate these problems is to identify somatic stem cells that can differentiate into hepatic lineages and use them for cell transplantation therapy. Recent studies have shown that somatic stem cells derived from the salivary gland, which are known as salivary gland progenitor (SGP) cells, can differentiate into hepatic or pancreatic cell lineages in rats and mice (Okumura et al., 2003; Hisatomi et al., 2004) as well as in pigs (Matsumoto et al., 2007). It is hoped that the isolation of SGP cells from patients with severe liver disease and their transplantation back into the patients will enable regeneration of their livers without immunorejection and the time-consuming search for matching donors.

To use SGP cells in human patients, it is important to establish protocols for their quality control, such as determining whether the cells are pure and whether they can differentiate appropriately. We are currently examining the use of SGP cells in regenerative medicine in pigs, which are widely used as a model of the human immune system due to the similar size and function of their organs (Kurome et al., 2005). A useful approach to use pigs to establish a model system for self-transplantation regenerative medicine would be to transfer the SGP nucleus to recipient cells, in order to replicate the pig genome and to artificially create disease states in the pig (Dwyer et al., 2002). So far, only major hepatic (e.g., albumin and alfa-fetoprotein) and pancreatic (e.g., glucagon and insulin) markers have been used to assess the differentiation state (Matsumoto et al., 2007), but the differentiation-dependent expression and function of

* Corresponding author. Phone: +81-84-936-2112 (4623);
Fax : +81-84-936-2459;
E-mail: yamaguti@bt.fubt.fukuyama-u.ac.jp
† These authors contributed equally to this work.
doi:10.2108/zsj.25.129

many proteins remain to be characterized. Furthermore, in the pig, even proteins expressed in organs have been poorly characterized. Therefore, a first step is to catalog the proteins expressed in organs, especially the salivary gland (source of SGP cells) and liver (destination of differentiated SGP cells). After that, protein expression profiles can be used to determine the differentiation state of SGP cells.

Traditionally, protein expression profiling has been performed by two-dimensional electrophoresis followed by mass spectrometry (MS) (Unwin et al., 2003). This approach, however, is not effective for identifying very acidic or basic, or very small or large, proteins. Recently, a high-throughput gel-free alternative called "shotgun proteomics" has been developed. This method involves enzymatic digestion of a complex mixture of proteins, followed by sorting the peptide fragments by one or more steps of chromatography followed by data dependent MS-MS analysis, and, finally, identification of the origin of the peptides by a database search (Kang et al., 2005; Kubota et al., 2005). This strategy has shown impressive capabilities for high-throughput protein identification in a variety of biological systems such as in human proteome analysis (Kang et al., 2005).

In this study, we analyzed the proteins expressed in porcine liver and salivary gland by using on-line two-dimensional nanoflow liquid chromatography/tandem mass spectrometry (2D LC-LC-MS-MS) based on the dual-trap method (Kang et al., 2005). The on-line 2D-LC method utilized a homemade pulled-tip capillary column (C18) and a dual-purpose trap packed with strong cation-exchange (SCX) resins. Here we present the results of this study and also discuss the usefulness of protein catalogs like those we obtained.

MATERIALS AND METHODS

Animals

Tissues were isolated from a crossbred (Large White/Landrace ×Duroc) barrow (52 d; 10.4 kg). After an 18-h fast, the barrow was anesthetized with atropine (0.2 mg/kg), azaperone (4 mg/kg), and ketamine (20 mg/kg) and killed by bleeding. Liver and salivary gland were rapidly collected, divided into approximately 1-g portions, frozen in liquid nitrogen, and stored at –80°C. All procedures were carried out in accordance with the Regulation of Experiments of the National Agricultural Research Center for Kyushu Okinawa Region (KONARC) and approved by the Animal Experiments Committee of KONARC.

Protein extraction from porcine liver and salivary gland

A piece of porcine liver or salivary gland was homogenized in extraction buffer (7 M urea, 2 M thiourea, 4% CHAPS, 50 mM dithiothreitol, and 0.1% SDS) containing a protease inhibitor cocktail (Sigma). The liver homogenates were centrifuged at 17,000×*g* for 30 min. at 4°C to remove cell debris, and the supernatant lysate was transferred to an Amicon YM-3 centrifugal filter unit (15 mL) having a membrane filter (3,000 molecular mass cutoff) from Millipore (Bedford, MA), to wash off the extraction buffer. The lysate was the retrieved by reverse filtration with 0.1 M phosphate buffer solution. Protein concentration was measured by the Bradford method (Bradford, 1976). Proteins extracted were stored at –80°C until use.

Sample clean up and protein digestion

Protein extracts from both porcine liver and salivary gland were digested and prepared by the following procedure. Approximately 100 μg of each lyophilized protein extract was dissolved in 0.1 M phosphate buffer containing 8 M urea and 10 mM dithiothreitol. After incubation of the solution at 37°C for 2 h, 20 mM iodoacetamide was added to alkylate the reduced thiol groups in the dark at 0°C for 2 h. Excess cystein (~40X) was added to remove the remaining iodoacetamide, and the mixture was diluted with phosphate buffer at a total concentration of 1.0 M urea. For digestion, proteomics-grade trypsin (Sigma; St. Louis, MO, USA) was added to the protein solution at 1:50 (protein:trypsin) and the mixture was incubated for 18 h at 37°C. At the end of digestion, alpha-tosyl-L-lysine chloromethyl ketone (TLCK) was added at a slight excess to the estimated number of moles of peptides. The final solution was cleaned up with an Oasis HLB cartridge (Waters; Milford, MA, USA) using acetonitrile, and the remaining organic solvent was evaporated in a vacuum centrifuge. The powdered peptides were redissolved in 5% CH_3CN in water containing 0.1% formic acid for 2D-LC-LC-MS-MS analysis.

2D-LC-LC-MS-MS

The on-line 2D-LC-LC-MS-MS system utilized in this study was based on the experimental setup reported previously (Kang et al., 2005). The 2D-LC consisted of an analytical column (C18-150 mm×75 μm i.d. (inner diameter)) and a dual trap column (SCX-15 mm and C18-10 mm×200 μm i.d.), as shown in Fig. 1. Both columns were made in-house with fused-silica capillaries (Polymicro Technology LLC; Phoenix, AZ, USA). Before packing the column, one end of the analytical column was pulled by flame into a tip diameter of about 10 μm, and the end tip was filled with frit about 2 mm in length, as explained by Kang et al. (2005). One end of the dual trap column was filled in the same way with frit about 2 mm in length. Both columns were packed in house: the analytical column was packed with Magic C18AQ™ resins having 5.0 μm-100 Å pore size (Michrom BioResources Inc.; Auburn, CA, USA), and the dual trap was packed with Magic C18AQ™ resins having 5.0 μm–200 Å in the first 1.0 cm, followed by packing for 1.5 cm with Polysulfoethyl A™ SCX resins having 5.0 μm–300 Å pore size (Nest Group Inc.; Southboro, MA, USA). The 2D-LC system was constructed by connecting both the dual trap column and analytical column with a PEEK microcross, and by directly interfacing the analytical column to MS via ESI as shown in Fig. 1. For the supply of electric voltage for ESI, a Pt wire was connected to the PEEK microcross. The 2D-LC-LC-MS-MS was carried out using the CapLC system (Waters; Milford, MA, USA), which consisted of three syringe pumps: two pumps for the binary gradient and another for delivering sample solution from the autosampler to the trap column, as shown in Fig. 1.

A sample of peptide mixture was initially loaded from the autosampler to the SCX part of the dual trap (the solid-line configuration of Fig. 1), and the bound peptides were eluted from SCX with NH_4HCO_3 solution. The SCX separation was made with a step gradient by increasing the concentration of the NH_4HCO_3 solution (0, 5, 10, 15, 20, 50, and 500 mM). Delivery of the NH_4HCO_3 solution, which was stored in a microvial of the autosampler, was made by pump C. The solution delivered by pump C was 5% CH_3CN with 0.1% formic acid. Only 8 μL of each salt solution was delivered to the SCX trap to elute bound peptides, and the desorbed peptides were readily absorbed by the C18 trap next to the SCX resins in the dual trap. When desorbed peptides were transferred to the C18 trap, desalting was made by delivery by pump C of the same solution used for sample delivery. During this process, all flow was directed toward the waste line via the PEEK microcross, due to the pressure from the analytical column. After desalting, the 10-port valve was turned to 36 degrees so that the binary gradient flow from pumps A and B could enter the analytical column with the vent line closed but with the split outlet open. In this configuration, only a small portion (180 nL/min) of pump flow was directed to the analytical column, and all remaining flow exited through the micro-Tee.

Binary gradient RPLC separation was carried out by varying the mobile phase composition of (A) 5% acetonitrile (ACN) in water and (B) 95% ACN. Both mobile phases contained 0.1% (v/v) formic acid. The gradient began with an increase from 0% B to 10% B over

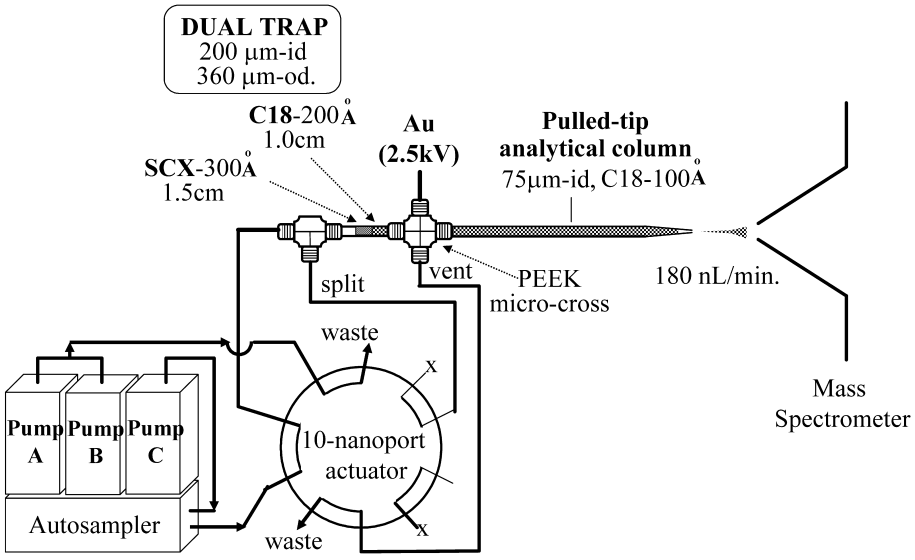

Fig. 1. A schematic illustration of the 2D-LC-LC-MS-MS experimental setup employed in this study. The homemade column configurations are explained in detail in Materials and Methods. The 10-port valve operation shown in the Fig. is for sample loading and salt step elution. During the RPLC run, the valve position needs to be turned to 36 degrees.

10 min and ramped to 18% for 10 min, to 30% B for 70 min, and to 80% B for 3 min. It was then maintained at 80% for 10 min to wash the column, decreased to 0% for 3 min, and maintained for at least 10 min for column reconditioning. The flow rate during the gradient separation was kept at 200 nL/min, and the eluted peptides were electrosprayed directly into the mass spectrometer.

MS analysis was made with a Q-TOF Ultima mass spectrometer from Waters using direct ESI from the nanoflow LC separation. ESI of peptides was achieved by applying a voltage of 1.8 kV through the Pt wire connected at the PEEK microcross. Eluting peptide ions were analyzed first by precursor scan (200~2000 amu), followed by three data-dependent tandem mass spectrometry runs using collision-induced dissociation (CID).

Data processing

MS-MS spectra obtained from Q-TOF MS were analyzed with the Mascot Search program against the Swiss-Prot database and MSDB. A protein search was initially made with the porcine database and then followed by one with the mammalian database. Some proteins identified as other than porcine were selected in the following limited cases. Only other mammalian proteins identified by more than two peptide hits were selected as equivalent porcine proteins. The mass tolerance between the measured monoisotopic mass and the selected mass was 1.5 u for the molar mass of a precursor peptide ion and 1.0 u for CID fragments. From the searched protein/peptide lists, only those peptides having a Mascot score larger than 30 were selected as showing extensive similarity at the 95% confidence level (Yang et al., 2004; Wan et al., 2006).

RESULTS

Samples of both peptide mixtures digested from the porcine liver and salivary gland proteomes were analyzed by 2D-LC-LC-MS-MS. For each sample, six different concentrations of salt solution (NH_4HCO_3) were applied for the salt step gradient of SCX separation, and after each elution of salt solution, a nanoflow LC run was carried out with data-dependent tandem MS spectrometric analysis. Including the breakthrough LC run made right after loading the sample onto the SCX resins of the dual trap, seven different RPLC runs were made for each proteome sample.

Fig. 2 shows a two-dimensional map of base peak chromatograms (BPCs) from nanoflow LC runs of porcine liver peptide mixture (5 μg) which were obtained at every salt step gradient along with each individual BPC. After sample loading onto the SCX part of the dual trap, a breakthrough run (RPLC) was carried out to detect some peptides that were neutral or not retained in the cation exchange resins. The breakthrough RPLC run in Fig. 2 shows a significant number of peaks. The broad peak at the end of elution (around 85 min) appeared to originate partly from the transition of the mobile phase composition of the binary gradient to the organic rich phase and partly from elution of some remaining surfactants used for cell lysis, but the contribution from the latter seemed to disappear in subsequent RPLC runs. However, not many proteins/peptides were identified from this breakthrough run, which represented numerous peaks apparently originating from some neutral small molecules or impurities.

After the breakthrough run, 8 μL of 5 mM NH_4HCO_3 solution were delivered to the SCX trap from the autosampler via pump C (see Fig. 1), and some peptides eluted from the SCX trap were transferred to the C18 part of the dual trap. A second RPLC gradient elution was then accomplished. The salt step elution-RPLC run cycle was repeated by increasing the salt concentration to 10, 15, 20, 25 mM NH_4HCO_3, and finally 500 mM solution was used to wash off all peptides remaining in the SCX resin. As shown in Fig. 2, many peptides peaks were observed at the 5 mM NH_4HCO_3 solution step, with very few apparent peaks in the rest of the runs. While not many peptide peaks were apparent in the RPLC run of 20 mM NH_4HCO_3, it was possible to obtain a number of peptide peaks solidly identified to proteins.

Fig. 3 shows the MS precursor scan at the retention time of 92.1 min of the 500 mM NH_4HCO_3 salt step elution (shown with the dotted line in Fig. 2) along with the data-dependent MS-MS spectrum of the ion having an m/z of 852.55. While the BPC after the 500 mM salt step elution

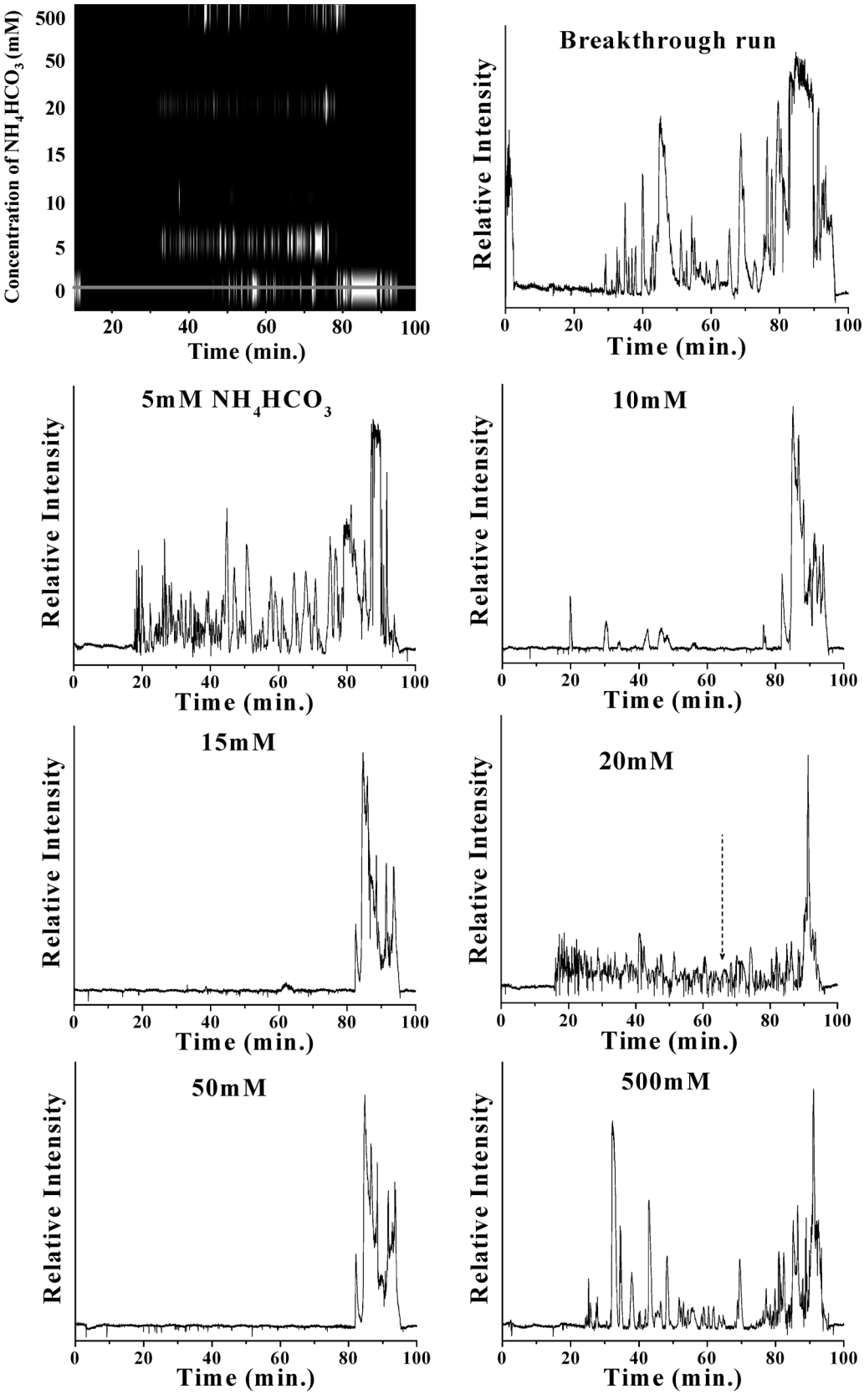

Fig. 2. Two-dimensional map of base peak chromatograms (RPLC) of porcine liver protein digests at different salt step cycles (different concentrations of NH_4HCO_3 solution). Peak intensities are represented by the brightness of white lines in the map, along with seven RPLC chromatograms obtained at each salt step elution. The breakthrough run was obtained right after the peptide mixtures were loaded into the dual trap. See text for experimental conditions of the binary gradient RPLC runs.

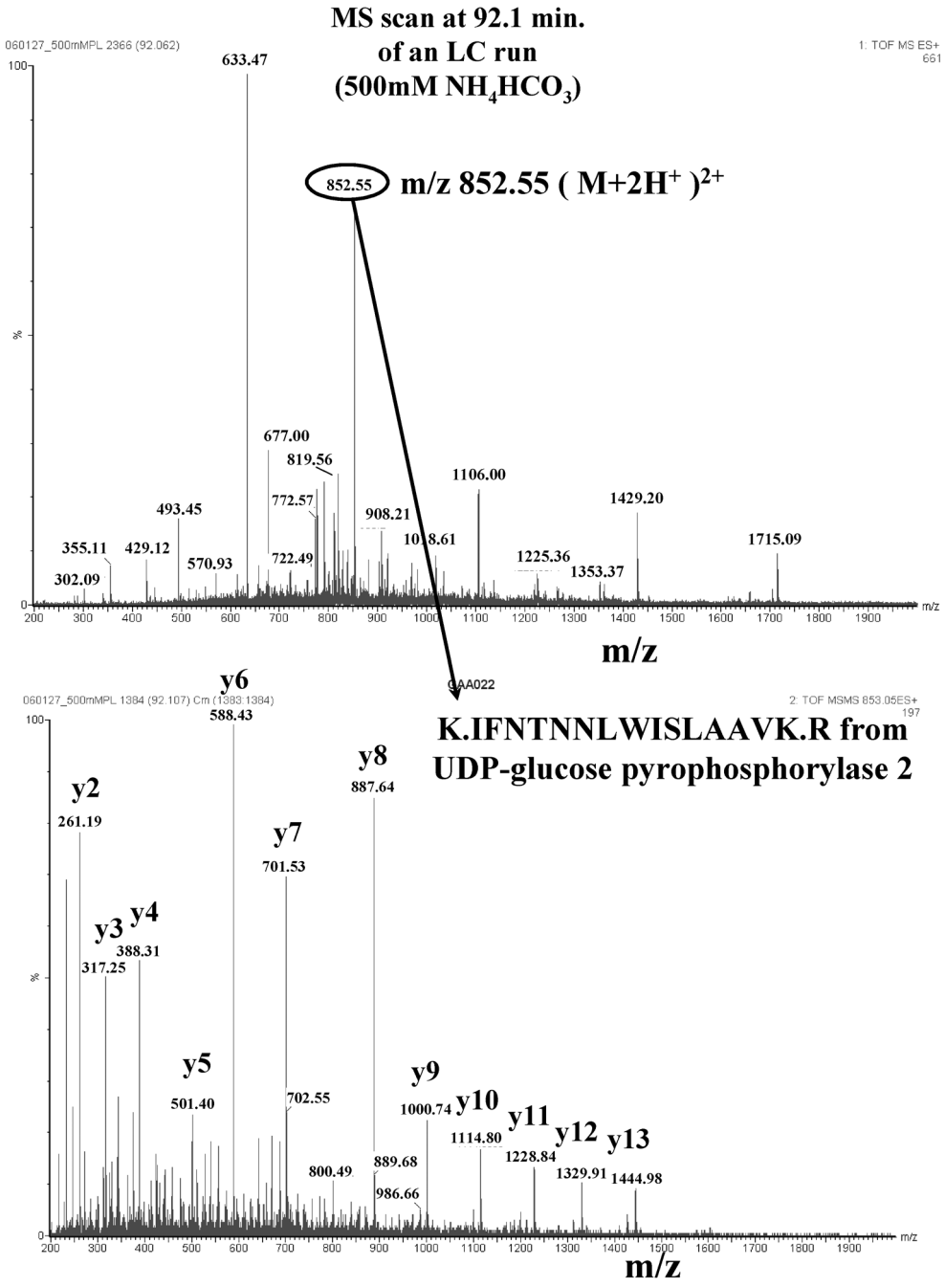

Fig. 3. Precursor MS scan of nanoflow LC effluent at 92.1 min of the salt step cycle at 500 mM NH_4HCO_3 from Fig. 2, along with the data-dependent collision induced fragmentation (CID) spectrum of the selected peptide ion, m/z=852.55 $(M+2H^+)^{2+}$. A database search resulted in the identification of UDP-glucose pyrophosphorylase 2 containing the peptide sequence K.IFNTNNLWISLAAVK.R.

shows a noisy baseline at around 92.1 min, the precursor scan shown in Fig. 3 shows numerous peaks. The data-dependent CID spectrum of m/z=852.55 $(M+2H^+)^{2+}$ followed by a database search resulted in identification of a peptide having sequence K.IFNTNNLWISLAAVK.R, originating from UDP- glucose pyrophosphorylase 2, which is a characteristic protein expressed in porcine liver.

The reproducibility of CID experiments on different batches of sample injection, in which a single injection included an entire salt step elution with each RPLC run, was fairly good, as shown previously (Kang et al., 2005). From seven RPLC-ESI-MS-MS experiments, we identified a total of 154 proteins, including 81 proteins from multiple peptide hits. The identified proteins are listed in Table 1. Some of the proteins in Table 1 are listed as from human or some other mammalian source, since the database search was carried out first against the porcine and then against the mammalian database. However, only proteins identified by multiple peptides were selected as equivalent to porcine proteins.

Fig. 4 shows the results obtained from the porcine

Table 1. Proteins identified in porcine liver.

Identified proteins in porcine liver					
Acc. No.	Identified protein	#	Acc. No.	Identified protein	#
P61603	10 kDa heat shock protein, mitochondrial_Bovine	3	Q94PW4	ATPase 8_Pig	1
P28037	10-formyltetrahydrofolate dehydrogenase_Rat	4	AAN15276	AY138843,mitochondrial_Bos taurus	9
O97509	14.3 kDa perchloric acid soluble protein_Goat	1	BHMT_PIG	Betaine-homocysteine S-methyltransferase_Pig	5
P62261	14-3-3 protein epsilon_Bovine	1	CRTC_PIG	Calreticulin_Pig	1
Q28956	17beta-estradiol dehydrogenase_Pig	2	Q8WN73	Carbamoyl-phosphate synthetase 1_Pig+Rat	6+11
1DUBA	2-enoyl-coa hydratase, chain A_Rat	1	S19307	* Carboxylesterase_Pig	6
O02691	3-hydroxyacyl-CoA dehydrogenase type II_Bovine	1	CATA_PIG	Catalase_Pig	8
DEPGC	3-hydroxyacyl-CoA dehydrogenase, short chain_Pig	1	COMT_PIG	Catechol-O-methyltransferase, soluble form_Pig	6
HPPD_PIG	4-hydroxyphenylpyruvate dioxygenase_Pig	1	KHPGD	Cathepsin D_Pig	1
Q9NZT7	4-trimethylaminobutyraldehyde dehydrogenase_Human	4	HHMS60	Chaperonin groEL_Mouse	4
P05386	60S acidic ribosomal protein P1_Rat	1	A29240	* Cofilin_Pig	1
RLA2_PIG	60S acidic ribosomal protein P2_Pig	1	Q9GKP1	Complement component C3_Pig	1
1KAY	70kd heat shock cognate protein atpase domain mutant K71A_Bovine	5	CYB5_PIG	Cytochrome B5_Pig	3
P11021	78 kDa glucose-regulated protein_Human	1	Q28977	Cytochrome P450 2C34v3_Pig	1
Q29092	* 94 kDa glucose-regulated protein_Pig	4	Q8SQ65	Cytochrome P450 2C49_Pig	1
Q9GKK0	Acetyl-coenzyme A acyltranferase_Pig	1	JC5819	Cytochrome P450 2D_Pig	1
ATBOB	* Actin beta_Bovine	10	Q8SQ64	Cytochrome P450 2E1_Pig	1
P79273	Acyl-CoA dehydrogenase, short-chain specific, mitochondrial_Pig	1	Q9XSG3	Cytosolic NADP+-dependent isocitrate dehydrogenase_Bovine	1
AAD02918	AF020038_Human	1	Q02338	D-beta-hydroxybutyrate dehydrogenase, mitochondrial_Human	2
AAF06698	AF047489_Human	1	Q9TV69	Dimeric dihydrodiol dehydrogenase_Pig	1
AAD25332	AF104312_Mouse	1	Q9DBT9	Dimethylglycine dehydrogenase, mitochondrial_Mouse	1
AAD38072	AF154830_Human	2	P13804	* Electron transfer flavoprotein alpha-subunit, mitochondrial_Human	4
Q9BYV1	Alanine--glyoxylate aminotransferase 2, mitochondrial_Human	1	P68103	Elongation factor 1-alpha 1_Bovine	11
ALDX_PIG	Alcohol dehydrogenase [NADP+]_Pig	2	P58252	Elongation factor 2_Mouse	2
ADHP_HUMAN	Alcohol dehydrogenase class II pi chain_Human	1	Q29092	Endoplasmin_Pig	3
S02302	Aldehyde dehydrogenase (NAD) 1, cytosolic_Horse	1	S06477	Enoyl-CoA hydratase, mitochondrial_Rat	1
1A4ZA	Aldehyde dehydrogenase (NAD+) 2, mitochondrial_Bovine	3	S57651	Enoyl-CoA hydratase/ 3-hydroxyacyl-CoA dehydrogenase, peroxisomal	1
Q8MI17	Aldehyde dehydrogenase 1A1_Rabbit	7	P79381	Epoxide hydrolase_Pig	1
Q9R146	Alpha actin_Pig	1	S45379	Fatty acid-binding protein, hepatic_Pig	1
NOA_HUMAN	Alpha enolase (2-phospho-D-glycerate hydro-lyase)_Human	3	Q923D2	Flavin reductase_Mouse	1
A54731	* Alpha-1 acid glycoprotein_Pig	1	P53603	Formimidoyltransferase-cyclodeaminase_Pig	3
FAHUAA	Alpha-actinin 1_Human	1	PAPGF	Fructose-bisphosphatase_Pig	5
ACY1_PIG	Aminoacylase-1_Pig	1	Q91Y97	Fructose-bisphosphate aldolase B_Mouse	5
P04272	Annexin A2_Bovine	1	P35505	Fumarylacetoacetase_Mouse	1
AOP2_BOVIN	Antioxidant protein 2_Bovine	1	P79315	GDP dissociation inhibitor beta_Pig	1
APA1_PIG	Apolipoprotein A-I precursor_Pig	1	NUPG	Glucose-6-phosphate isomerase_Pig	2
B46018	Apolipoprotein C-III_Pig	1	S39010	Glutamate dehydrogenase [NAD(P)]_Pig+Rat	1+1
AJHURS	Argininosuccinate synthase_Human	3	GTA1_PIG	Glutathione S-transferase alpha M14_Pig	6
XNPGDM	Aspartate transaminase, mitochondrial_Pig	2	Q29581	Glutathione transferase_Pig	1
ATPK_BOVIN	ATP synthase f chain, mitochondrial_Bovine	1	Q8BH04	Phosphoenolpyruvate carboxykinase, mitochondrial_Mouse	2
G3P_PIG	Glyceraldehyde 3-phosphate dehydrogenase_Pig	4	AAA31120	PIGSCOA_Pig	1
Q9Y6B6	GTP-binding protein SAR1b_Human	1	1QPWB	Poricine hemoglobin (beta subunit), chain B_Pig	7
Q9T2U6	H+-ATPase subunit, OSCP=OLIGOMYSIN sensitivity conferring protein_Pig	1	Q92620	Pre-mRNA splicing factor ATP-dependent RNA helicase PRP16_Human	1
PWBOB	H+-transporting two-sector ATPase beta chain, mitochondrial_Bovine	6	1AWIA	* Profilin, chain A_Human	2
PWBOA	H+-transporting two-sector ATPase, alpha chain precursor, cardiac_Bovine	4	FABO	* Profilin_Bovine	2
Q96FZ6	Heat shock 60kD protein 1_Human	9	A39682	Prohibitin_Rat	1
Q9DC41	Heat shock 70kD protein 5_Mouse	4	A25516	Propionyl-CoA carboxylase, beta chain_Rat	1
HHHU27	Heat shock protein 27_Human	1	A28396	Prostaglandin-F synthase_Bovine	1
HS9A_PIG	* Heat shock protein HSP 90-alpha_Pig	9	Q15084	Protein disulfide-isomerase A6_Human	1
1NGB	Heat-shock cognate 70kd protein mutant with glu 175	2	JC2385	Protein disulfide-isomerase ER60_Bovine	4
HAPG	Hemoglobin alpha chain_Pig	4	ISBOSS	Protein disulfide-isomerase_Bovine	3
HBB_PIG	* Hemoglobin beta chain_Pig	1	1BOH	Rhodanese_Bovine	1
HBE_PIG	Hemoglobin epsilon chain_Pig	1	Q9GMB0	* Ribophorin I_Pig	1
HSHUA1	* Histone H2A.1_Human	1	P31153	S-adenosylmethionine synthetase gamma form_Human	1
HSBO2A	Histone H2A_Bovine	3	SAP_PIG	Saposin B_Pig	2
HSBO22	Histone H2B_Bovine	3	S72173	Senescence marker protein 30_Mouse+Rabbit	3
P62802	* Histone H4_Pig	3	Q9UBB1	Sepiapterin reductase	1
Q8R3H3	Hypothetical 14.5 kDa protein	1	ABPGS	* Serum albumin_Pig	7
Q8TED6	Hypothetical protein FLJ23617_Human	1	Q9MYP6	Short-chain dehydrogenase/reductase_Bovine	2
CAC86339	Immunoglobulin gamma 3 heavy chain constant region_Horse	1	Q969Z8	Solute carrier family 1, member 7_Human	1
Q95M34	Immunogobulin gamma 1 heavy chain_Horse	2	DHSO_RAT	Sorbitol dehydrogenase_Rat +Sheep	5
O75874	Isocitrate dehydrogenase [NADP] cytoplasmic_Human	2	Q9HCU6	Spermatogenic cell-specific glyceraldehyde 3-phosphate dehydrogenase-2_Human	1
IDI1_HUMAN	Isopentenyl-diphosphate delta-isomerase_Human	2	P48721	Stress-70 protein, mitochondrial_Rat	2
3HDHA	L-3-hydroxyacyl coa dehydrogenase, chain A_Pig	3	JC2258	Substrate protein of mitochondrial ATP-dependent proteinase SP-22_Bovine	2
Q9UQF9	Lysophospholipase isoform_Human	1	P31040	* Succinate dehydrogenase [ubiquinone] flavoprotein subunit, mitochondrial_ Human	1
Q9TUM7	Macrophage migration inhibitory factor_Pig	2	A44529	Succinate-CoA ligase (GDP-forming), beta chain_Pig	1
MDHC_PIG	* Malate dehydrogenase, cytoplasmic_Pig	2	DSPGCZ	* Superoxide dismutase_Pig	3
MDHM_PIG	Malate dehydrogenase, mitochondrial_Pig	9	THIO_PIG	Thioredoxin_Pig	1
3MDDA	Medium chain acyl-coa dehydrogenase, chain A_Pig	3	THTR_HUMAN	Thiosulfate sulfurtransferase_Human	1
MAPR_PIG	Membrane associated progesterone receptor component_Pig	1	S01384	Transferrin_Pig	5
Q95JB5	Mitochondrial 2,4-dienoyl-CoA reductase_Pig	1	VPPG	* Transitional endoplasmic reticulum ATPase_Pig	2
Q9ESE4	Olfactory UDP glucuronosyltransferase_Human	1	Q29554	* Trifunctional enzyme alpha subunit, mitochondrial_Pig	3
Q99497	Oncogene DJ1_Human	1	TPIS_RAT	* Triosephosphate isomerase_Rat	3
O19072	Ornithine carbamoyltransferase, mitochondrial_Pig	2	UBPGA	* Tubulin alpha chain_Pig	1
P62936	* Peptidyl-prolyl cis-trans isomerase A_Pig	4	P99024	Tubulin beta-5 chain_Mouse	5
Q9GLW8	* Peroxiredoxin 5_Pig	2	P12378	UDP-glucose 6-dehydrogenase_Bovine	2
1A44	Phosphatidylethanolamine-binding protein_Bovine+Human	1+1	UDP2_PIG	UTP--glucose-1-phosphate uridylyltransferase 2_Pig	3

*Those proteins identified in both organs are marked in both tables.

# indicates the number of peptides used to identify each protein.

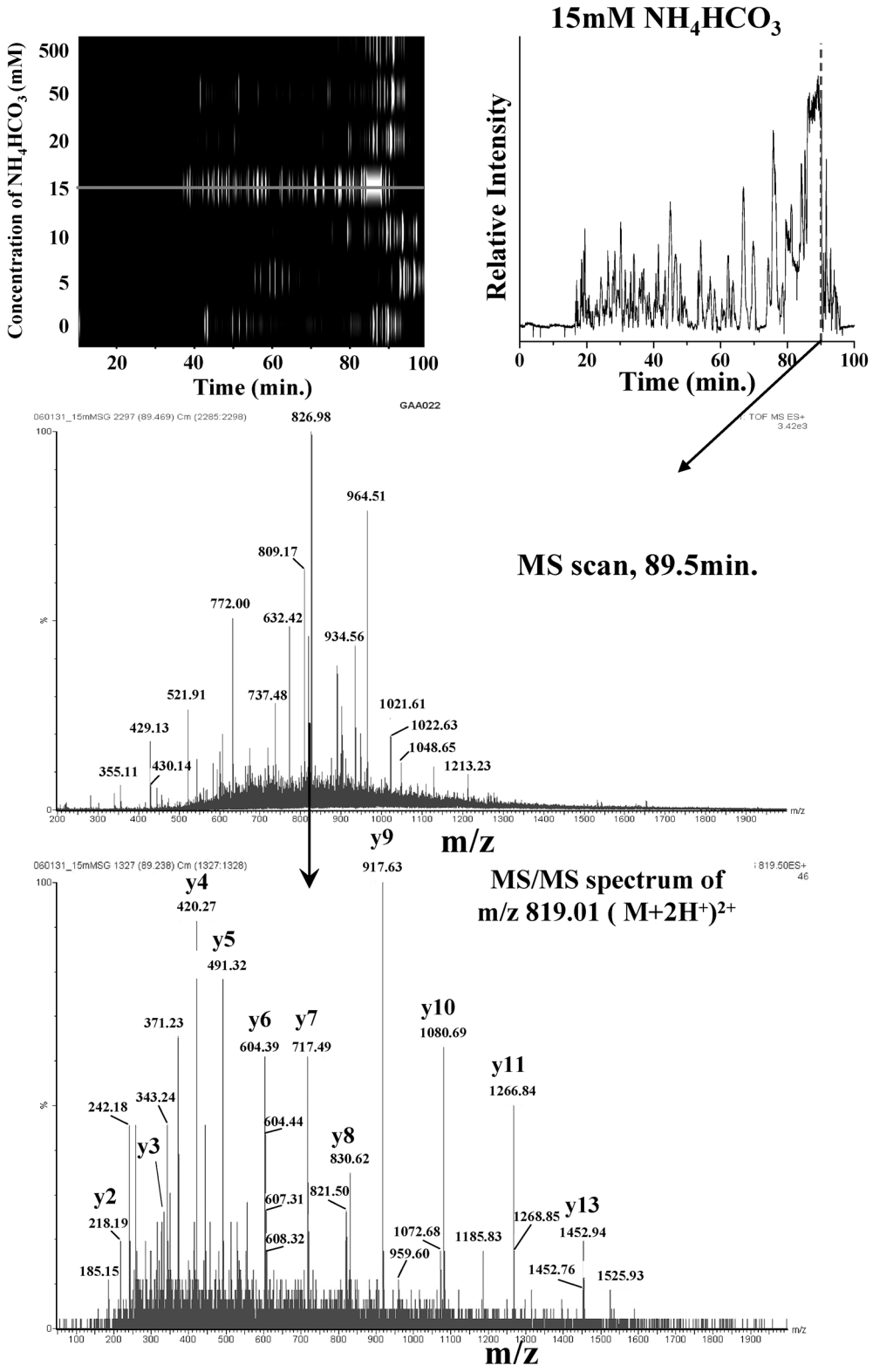

Fig. 4. Two-dimensional map of base peak chromatograms (RPLC) of porcine salivary gland protein digests at seven different salt step cycles, the BPC after the salt step cycle of 15 mM NH_4HCO_3 solution, a precursor MS scan at 89.5 min (represented by the dotted line in the BPC), and the corresponding data-dependent CID spectrum of the peptide ion having m/z of 819.01 $(M+2H^+)^{2+}$. A database search of the CID spectrum resulted in identification of the peptide sequence K.IAGEWYSILLASDAK.A originating from porcine salivary lipocalin.

salivary gland proteome: a 2D map of BPCs at different concentrations of NH_4HCO_3 solution, an example of BPC at the 15 mM NH_4HCO_3 cycle, a characteristic MS scan at 89.5 min (expressed by the dotted line in the BPC) of the salt cycle of 15 mM NH_4HCO_3, and the corresponding data-dependent CID spectrum of m/z 819.01 ($M+2H^+$) from the precursor scan. The peptide sequence identified from the database search was K.IAGEWYSILLASDAK.A [*m/z* 819.01, $(M+2H^+)^{2+}$], from porcine salivary lipocalin. Database searches for all LC-MS-MS experiments for porcine salivary gland ended up with a total of 117 proteins, including 37 proteins having multiple peptide hits. These are listed in Table 2.

Table 2. Identified proteins list in porcine salivary gland.

Identified proteins in porcine salivary gland					
Accession	Identified protein	#	Accession	Identified protein	#
P61604	10 kDa heat shock protein, mitochondrial_Human	1	Q8N473	Hypothetical protein_Human	2
P63104	14-3-3 protein zeta/delta_Human	1	P33198	Isocitrate dehydrogenase [NADP], mitochondrial_Pig	2
Q99714	3-hydroxyacyl-CoA dehydrogenase type II_Human	1	Q29550	Liver carboxylesterase_Pig	1
RL11_PIG	60S ribosomal protein L11_Pig	1	DEPGLH	L-lactate dehydrogenase, chain H_Pig	1
GRP78_HUMAN	78 kDa glucose-regulated protein_Human	5	P51884	Lumican_Human	1
1B0JA	Aconitate hydratase, mutant YES_Pig	1	MIF_PIG	Macrophage migration inhibitory factor_Pig	1
ATBOB	* Actin beta_Bovine	7	MDHC_PIG	*Malate dehydrogenase, cytoplasmic_Pig	2
Q6QRN9	ADP,ATP carrier protein 3_Pig	2	DEPGMM	Malate dehydrogenase, mitochondrial_Pig	4
P50578	Alcohol dehydrogenase [NADP+]_Pig	1	T03099	Mucin, submaxillary_Pig	3
P06733	Alpha enolase_Human	3	JX0215	Myosin catalytic light chain LC17b_Pig	1
A54731	* alpha-1 acid glycoprotein_Pig	1	P35579	Myosin heavy chain, nonmuscle type A_Human	1
P29700	Alpha-2-HS-glycoprotein_Pig	1	B24862	Na+/K+-exchanging ATPase, alpha chain_Pig	8
O43707	Alpha-actinin 4_Human	1	A24862	Na+/K+-exchanging ATPase, beta chain_Pig	2
ANX2_PIG	Annexin II_Pig	1	P42028	NADH-ubiquinone oxidoreductase 23 kDa subunit, mitochondrial_Bovine	1
AQHUP	Annexin V_Human	1	Q9TSX9	Non-selenium glutathione phospholipid hydroperoxide peroxidase_Pig	1
O95994	Anterior gradient protein 2 homolog_Human	1	JC4369	P5 protein_Human	2
Q95JC8	Arginase I_Pig	1	P62936	* Peptidyl-prolyl cis-trans isomerase A_Pig	2
P33097	Aspartate aminotransferase, cytoplasmic_Bovine	1	P23284	Peptidyl-prolyl cis-trans isomerase B_Human	2
XNPGDM	Aspartate transaminase, mitochondrial_Pig	1	Q9GLW8	* Peroxiredoxin 5, mitochondrial_Pig	1
ATPB_RAT	ATP synthase beta chain, mitochondrial_Rat	4	Q00325	Phosphate carrier protein, mitochondrial_Human	1
P30049	ATP synthase delta chain, mitochondrial_Human	1	PMGB_HUMAN	Phosphoglycerate mutase, brain form_Human	2
S06492	Beta-Galactoside-binding lectin_Pig	2	Q9H361	Polyadenylate-binding protein 3_Human	1
A56785	Calmodulin_Pig	1	1AWIA	* Profilin, chain A_Human	1
Q08092	Calponin-1_Pig	1	FABO	* Profilin_Bovine	1
P28491	Calreticulin_Pig	1	JC5260	Progesterone membrane binding protein_Pig	1
S19307	* Carboxylesterase_Pig	1	JC5704	Protein disulfide-isomerase, ER60_Human	4
A32800	Chaperonin GroEL_Human	1	Q9NTK5	Putative GTP-binding protein PTD004_Human	1
P35604	Coatomer zeta-1 subunit_Bovine	1	P62834	Ras-related protein Rap-1A_Human	1
A29240	* Cofilin_Pig	3	A45009	Rho protein GDP-dissociation inhibitor_Bovine	1
CGHU3A	Collagen alpha 3(VI) chain_Human	1	Q9GMB0	* Ribophorin I_Pig	2
Q8N1E1	Creatine kinase, mitochondrial 2_Human	1	P81608	Salivary lipocalin_Pig	5
P20674	Cytochrome c oxidase polypeptide Va, mitochondrial_Human	1	P09571	Serotransferrin_Pig	1
A27077	DnaK-type molecular chaperone_Human	3	ABPGS	* serum albumin_Pig	9
P13804	* Electron transfer flavoprotein alpha-subunit, mitochondrial_Human	1	Q61425	Short chain 3-hydroxyacyl-CoA dehydrogenase, mitochondrial_Mouse	1
P13639	Elongation factor 2_Human	1	Q9NR45	Sialic acid synthase_Human	1
T09549	Endoplasmic-reticulum-lumenal protein 28_Human	1	O14729	Smooth muscle myosin heavy chain SM2_Human	1
Q29092	* Endoplasmin_Pig	3	P05027	Sodium/potassium-transporting ATPase beta-1 chain_Pig	1
S22395	Fetuin_Pig	1	P31040	* Succinate dehydrogenase flavoprotein subunit, mitochondrial_Human	1
ALFA_RAT	Fructose-bisphosphate aldolase A_Rat	2	DSPGCZ	* Superoxide dismutase_Pig	2
Q9NZS6	Glucocorticoid receptor AF-1 specific elongation factor_Human	2	Q9Y490	Talin 1_Human	1
GFA1_HUMAN	Glucosamine-fructose-6-phosphate aminotransferase_Human	1	P82460	Thioredoxin_Pig	1
P50309	Glucose-6-phosphate isomerase_Pig	1	P37802	Transgelin-2_Human	1
GTP_PIG	Glutathione S-transferase P_Pig	1	VPPG	* Transitional endoplasmic reticulum ATPase_Pig	1
DEPGG3	Glyceraldehyde-3-phosphate dehydrogenase_Pig	2	P29401	Transketolase_Human	1
GRP78_HUMAN	H+-transporting two-sector ATPase, alpha chain_Bovine	7	EFHU1	Translation elongation factor eEF-1 alpha-1 chain_Human	1
P19120	Heat shock cognate 71 kDa protein_Bovine	3	Q29554	* Trifunctional enzyme alpha subunit, mitochondrial_Pig	1
HS9A_PIG	* Heat shock protein HSP 90-alpha_Pig	1	TPIS_RAT	* Triosephosphate isomerase_Rat	2
P04792	Heat-shock protein beta-1_Human	1	P67937	Tropomyosin alpha 4 chain_Pig	1
P01965	Hemoglobin alpha chain_Pig	1	Q8WU19	Tubulin alpha 2_Human	3
HBB_PIG	* Hemoglobin beta chain_Pig	5	UBPGA	* Tubulin alpha chain_Pig	2
P52597	Heterogeneous nuclear ribonucleoprotein F_Human	1	Q9BQE3	Tubulin alpha-6 chain_Human	1
P61978	Heterogeneous nuclear ribonucleoprotein K_Human	1	UBPGB	Tubulin beta chain_Pig	4
P14866	Heterogeneous nuclear ribonucleoprotein L_Human	1	P68371	Tubulin beta-2 chain_Human	1
P22626	Heterogeneous nuclear ribonucleoproteins A2/B1_Human	2	O60701	UDP-glucose 6-dehydrogenase_Human	2
Q00839	Heterogenous nuclear ribonucleoprotein U_Human	1	O75396	Vesicle trafficking protein SEC22b_Human	1
HSHUA1	* Histone H2A.1_Human	1	P02543	Vimentin_Pig	1
Q29579	Histone H2B and H2A_Pig	1	P45880	Voltage-dependent anion-selective channel protein 2_Human	1
HSHUB1	Histone H2B.1_Human	1	H2BC_HUMAN	Histone H2B.c_Human	1
P62802	* Histone H4_Pig	1			

DISCUSSION

In this study, we performed a large-scale protein identification by shotgun proteomics of the porcine salivary gland (a source of SGP cells) and liver (a destination for differentiated SGP cells), and identified 117 and 154 proteins, respectively. To our knowledge, this is the first report of large-scale protein catalogs for porcine organs.

Of the proteins identified in the two proteomes, 45 were redundant, whereas many others were specific to each organ (109 specific to liver and 72 specific to salivary gland). Among liver-specific proteins, there were some housekeeping proteins, and there were several others already reported to be abundantly expressed in liver, including catalase, cytochrome P450, and ornithine carbamoyltransferase (Lin et al., 1997; Baranova et al., 2005; Koger and Jones, 1997). Likewise, among the salivary gland-specific proteins, we identified some predicted to function in the salivary gland or saliva, such as submaxillary apomucin and salivary lipocalin precursor (Eckhardt et al., 1997; Loebel et al., 2000). Although we did not identify a high number of organ-specific proteins, comparison of the proteomes of salivary gland, liver, and differentiated SGP may allow determination of the state of SGP differentiation. Analysis of the SGP proteome remains to be carried out, and it will be necessary to expand the proteome map for both liver and salivary gland, because the accuracy of quality-control analysis is enhanced by identification of increased numbers of tissue-specific proteins. Because cells are predicted to contain thousands of proteins across a wide concentration range, prefractionation and additional protein extraction methods may be required.

The quality control of SGP differentiation (i.e., to determine whether SGPs are differentiating appropriately) can also be enhanced by comparison with the proteomes of additional organs. For this purpose, proteome maps should be created for all porcine organs using the method described in the current study to select markers for each organ. Identification of useful marker proteins could be improved by performing not only the qualitative analysis described here but also quantitative analysis, for example by using ICAT or iTRAQ reagents (Dunkley et al., 2004; DeSouza et al., 2005).

Although we identified expected tissue-specific proteins, we observed some unexpected expression patterns. For instance, alpha-2-HS-glycoprotein precursor was previously known to be expressed mostly by the liver and to be secreted into the serum (Brown et al., 1992), but we identified it in the salivary gland proteome. Other liver markers, such as albumin, alcohol dehydrogenase, and arginase I, were also identified in the salivary gland proteome. These unexpected findings of liver-specific proteins in the salivary gland suggest two possibilities: (i) the proteins are delivered to the salivary gland by the blood stream or are contaminants of the salivary tissue with blood components, or (ii) the proteins are normally expressed in the salivary gland. With respect to the latter possibility, it is possible that proteins are expressed in both organs because these organs are both derived from the endoderm. This also is consistent with the fact that somatic stem cells isolated from the salivary gland can transform into a hepatic lineage.

In addition to the usefulness of proteome maps for assessing the state of SGP differentiation, they are also useful for comparison with the human proteome. Porcine organs have been extensively studied for use in xenotransplantation to humans because they have similar sizes and physiological functions (Kurome et al., 2005). Most of the previous work in this area has focused on the elimination of hyperacute immunorejection and porcine endogenous retroviruses (Takeuchi et al., 2005). To achieve xenotransplantation from pig to human, however, it will be necessary to compare the expression and function of proteins in both species. The protein catalogs obtained here should help in this regard.

ACKNOWLEDGMENTS

We are grateful to Fumio Endo for sharing his unpublished results. We also thank to Jun J. Sato for critical reading of the manuscript. This study was supported by the Program for Promotion of Basic Research Activities for Innovative Biosciences (PROBRAIN). MHM also thanks the Korea Science and Engineering Foundation through the Center for Bioactive Molecular Hybrids (CBMH) at Yonsei University.

REFERENCES

Baranova J, Anzenbacherova E, Anzenbacher P, Soucek P (2005) Minipig cytochromo P450 2E1: comparison with human enzyme. Drug Metab Dispos 33: 862–865

Bradford MM (1976) A rapid and sensitive method for the quantitation of microgram quantities of protein utilizing the principle of protein-dye binding. Anal Biochem 72: 248–254

Brown KA, Moonka D (2004) Liver transplantation. Curr Opin Gastroenterol 20: 264–269

Brown WM, Dziegielewska KM, Saunders NR, Christie DJ, Nawratil P, Muller-Esterl W (1992) The nucleotide and deduced amino acid structures of sheep and pig fetuin. Common structural features of the mammalian fetuin family. Eur J Biochem 205: 321–331

DeSouza L, Diehl G, Rodrigues MJ, Guo J, Romaschin AD, Colgan TJ, Siu KW (2005) Search for cancer markers from endometrial tissues using differentially labeled tags iTRAQ and cICAT with multidimensional liquid chromatography and tandem mass spectrometry. J Proteome Res 4: 377–386

Dunkley TP, Dupree P, Watson RB, Lilley KS (2004) The use of isotope-coded affinity tags (ICAT) to study organelle proteomes in *Arabidopsis thaliana*. Biochem Soc Trans 32: 520–523

Dwyer KM, Cowan PJ, d'Apice AJ (2002) Xenotransplantation: past achievements and future promise. Heart Lung Circ 11: 32–41

Eckhardt AE, Timpte CS, DeLuca AW, Hill RL (1997) The complete cDNA sequence and structural polymorphism of the polypeptide chain of porcine submaxillary mucin. J Biol Chem 272: 33204–33210

Hisatomi Y, Okumura K, Nakamura K, Matsumoto S, Satoh A, Nagano K, Yamamoto T, Endo F (2004) Flow cytometric isolation of endodermal progenitors from mouse salivary gland differentiate into hepatic and pancreatic lineages. Hepatology 39: 667–675

Kang D, Nam H, Kim Y, Moon MH (2005) Dual-purpose sample trap for on-line strong cation-exchange chromatography/reversed-phase liquid chromatography/tandem mass spectrometry for shotgun proteomics. Application to the human Jurkat T-cell proteome. J Chromatogr A 1070: 193–200

Kellum JA, Bellomo R, Mehta R, Ronco C (2003) Blood purification in non-renal critical illness. Blood Purif 21: 6–13

Koger JB, Jones EE (1997) Nucleotide sequence of porcine OTCase cDNA. J Anim Sci 75: 3368

Kubota K, Kosaka T, Ichikawa K (2005) Combination of two-

dimensional electrophoresis and shotgun peptide sequencing in comparative proteomics. J Chromatogr B 815: 3–9

Kurome M, Ueda H, Tomii R, Nakamura K, Okumura K, Matsumoto S, Endo F, Nagashima H (2005) Production of cloned pigs from somatic stem cells derived from salivary gland. Reprod Fert Develop 17: 170

Lin ZH, Wang YF, Sarai A, Yasue H (1997) Swine catalase deduced from cDNA and localization of the catalase gene on swine chromosome 2p16-p15. Biochem Genet 35: 297–302

Loebel D, Scaloni A, Paolini S, Fini C, Ferrara L, Breer H, Polosi P (2000) Cloning, post-translational modifications, heterogenous expression and ligand-binding of boar salivary lipocalin. Biochem J 350: 369–379

Matsumoto S, Okumura K, Ogata A, Hisatomi Y, Sato A, Hattori K, Matsumoto M, Kaji Y, Takahashi M, Yamamoto T, Nakamura K, Endo F (2007) Isolation of tissue progenitor cells from duct-ligated salivary glands of swine. Cloning Stem Cells 9: 176–190

Naruse K (2005) Artificial liver support: future aspects. J Artif Organs 8: 71–76

Okumura K, Nakamura K, Hisatomi Y, Nagano K, Tanaka Y, Terada K, Sugiyama T, Umeyama K, Matsumoto K, Yamamoto T, Endo F (2003) Salivary gland progenitor cells induced by duct ligation differentiate into hepatic and pancreatic lineages. Hepatology 38: 104–113

Sarlis NJ, Gourgiotis L (2005) Hormonal effects on drug metabolism through the CYP system: perspectives on their potential significance in the era of pharmacogenomics. Curr Drug Targets Immune Endocr Metabol Disord 5: 439–448

Shimada M, Fujii M, Morine Y, Imura S, Ikemoto T, Ishibashi H (2005) Living-donor liver transplantation: present status and future perspective. J Med Invest 52: 22–32

Takeuchi Y, Magre S, Patience C (2005) The potential hazards of xenotransplantation: an overview. Rev Sci Tech 24: 323–334

Unwin RD, Gaskell SJ, Evans CA, Whetton AD (2003) The potential for proteomic definition of stem cell populations. Exp Hematol 31: 1147–1159

Wan Y, Yang A, Chen T (2006) PepHMM: A hidden Markov model based scoring function for mass spectrometry database search. Anal Chem 78: 432–437

Yang X, Dondeti V, Dezube R, Maynard DM, Geer LY, Epstein J, Chen X, Markey SP, Kowalak JA (2004) DBParser: Web-Based Software for Shotgun Proteomic Data Analyses. J Proteome Res 3: 1002–1008

(Received May 20, 2007 / Accepted October 10, 2007)